The International Journal of Advanced Manufacturing Technology (2021) 114:97–105
https://doi.org/10.1007/s00170-020-06457-6

ORIGINAL ARTICLE

An analytical model for micro-cutting considering the cutting tool edge radius effect and material separation

Yiquan Li[1] · Zhanjiang Yu[1] · Jinkai Xu[1] · Xiaozhou Li[1] · Huadong Yu[1]

Received: 3 July 2020 / Accepted: 1 December 2020 / Published online: 8 March 2021

Abstract

Severe plastic deformation occurs in micro metal cutting process; meanwhile, new surfaces are generated due to the material separation caused by ductile fracture. The energy required for the formation of the new surfaces is of kJ/m^2, which should not be neglected in the analysis of micro-cutting. In this work, an analytical model is developed focusing on the analyses of the micro metal cutting process with no stable built-up edge, in which the effects of both edge radius and material separation are taken into account. The cutting tool edge geometry is simplified with the effective rake angle. On the basis of slip-line field theory, the equation of the cutting power is derived. Applying the minimum energy principle, two nonlinear equations are obtained, through which the shear angle and the minimum chip thickness can be estimated simultaneously. The model is examined through the experiments; the investigations show that the calculation results of cutting force and shear angle agreed with the experimental measurements very well. The effects of fracture toughness, shear yield stress, and friction angle to the micro-cutting process are investigated. The numerical results show that the friction angle affects the cutting force and the shear angle greatly.

Keywords Micro-cutting · Cutting tool edge radius · Fracture toughness · Material separation

1 Introduction

Micro-cutting has extensive applications in the manufacturing of 3D miniature components with desired durability, strength, and surface quality using metals or composites [1–3]. In micro-cutting, the uncut chip thickness is comparable in size with the cutting tool edge radius. This gives rise to a negative rake angle, which significantly affects the cutting force, materials, the deformation, and the tool wear.

Tremendous efforts have been devoted in analyzing micro-cutting process theoretically, numerically or experimentally. Kim et al. [4] suggested an orthogonal cutting model considering the cutting tool edge radius and the elastic recovery and investigated the plowing along the rounded edge and the sliding on the clearance face. Liu et al. [5] developed a finite element model based on strain gradient plasticity to examine the size effect, which was attributed to the tool edge radius and length scale of the material. Lai et al. [6] also performed FE simulations for micro-scale orthogonal machining considering the material strain gradient strengthening behavior, the tool edge radius and the fracture of the material. Subbiah et al. [7] observed material separation through a series of experiments and found that ductile fracture occurred due to finite inserts radii. Afazov et al. [8] presented an approach for predicting micro-milling cutting forces using FEM considering the effects of the cutting tool edge radius and the run-out. Vipindas et al. [9] investigated the effect of the cutting tool edge radius on the cutting force, the coefficient of friction, the surface roughness, and chip formation during micro end milling. Wu et al. [10] developed a comparison method to calculate the plowing force in micro-cutting by considering the cutting tool edge radius. Jun et al. [11] proposed a mechanistic model of micro end milling forces, with consideration of the effects of plowing, elastic recovery, effective rake angle, and flank face rubbing. An et al. [12] proposed a new deburring method in the study of ultraprecision micro-cutting. Due to the complexity of the micro-cutting process, considerable works were focusing on the FEM simulation to study the stress field, the large plastic deformation and the cutting force, etc. [8, 13–19].

✉ Huadong Yu
yuhuadong@cust.edu.cn

[1] School of Mechatronical Engineering, Changchun University of Science and Technology, Changchun 130022, China

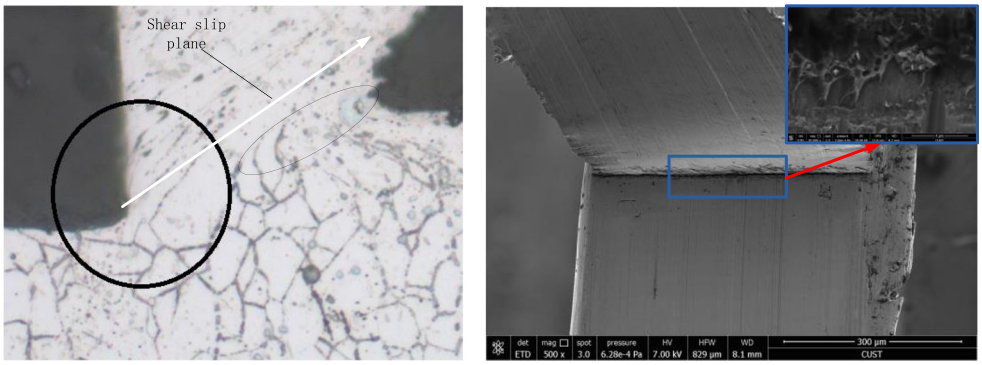

Fig. 1 SEM images of the chip root illustrating: **a** severe plastic deformation and **b** ductile fracture

A number of studies have been reported on the analytical and mechanistic models of micro-cutting process, based on slip-line field theory considering the effects of the cutting tool edge radius. Annoni et al. [20] used a slip-line field model to predict the cutting and the feed force based on the Waldorf model [21] under micro-scale cutting conditions considering effective rake angle. Jin et al. [22] established a slip-line field model to analyze the micro-cutting process with round edge. Fang [23, 24] proposed a slip-line model for the machining with a rounded-edge tool which consists of 27 slip-line sub-regions, each sub-region having its own physical meaning. It is noted that none of the above analytic models considered the material separation in cutting process.

In actual cutting process the work-piece material is removed by way of separation to form new surfaces. The creation of the new surfaces means that a portion of the work done by the cutting force in the cutting process is converted to surface energy. The specific surface work required is on the order of J/m^2 for the formation of a new surface as calculated by the surface chemical free energy, which can be neglected in the calculation of the power consumption [25]. Based on this view, the traditional cutting force and shear angle analysis model only considers the work consumed by the plastic deformation and friction. However, the work required to produce a new surface in the analysis of the fracture behavior of the material is much higher, and the work per unit area required for the crack propagation during the metal ductile fracture can reach several hundred kJ/m^2 [26]. Solid surface energy involves in the elastic and plastic deformation, cannot follow the definition for the free surface of the liquid. Thus, the surface chemical free energy is not suitable as a parameter characterizing the cutting process [27]. On the basis of the above considerations, the Ernst–Merchant cutting model has been modified applying the ductile fracture mechanics [28], and the interaction between cutting tool edge radius and material separation in micro-cutting process has been investigated using this methodology [29]. However, only the situation with a stable built-up edge was considered in [29], while in actual cutting process stable built-up edge may not generate under certain cutting conditions.

In this work, we proposed an analytical model of micro-cutting considering the factors of plastic flow, friction and ductile fracture, which can be used to estimate the shear angle and the material separation point position simultaneously. It should be pointed out that in the model no stable built-up edge is included.

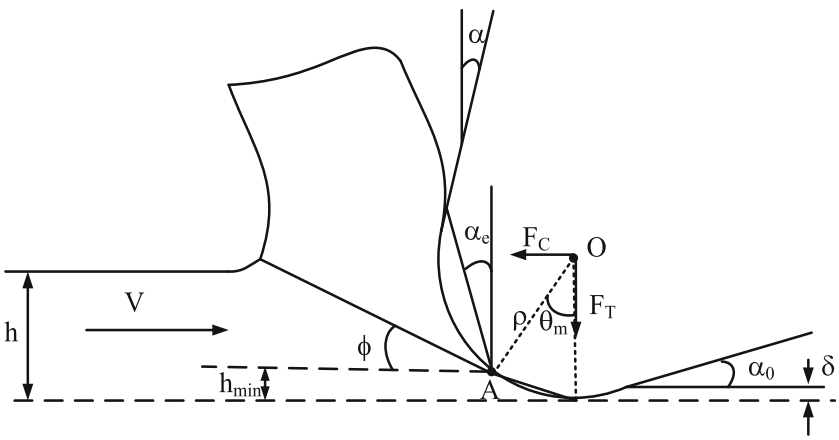

Fig. 2 Analysis model for micro-cutting process

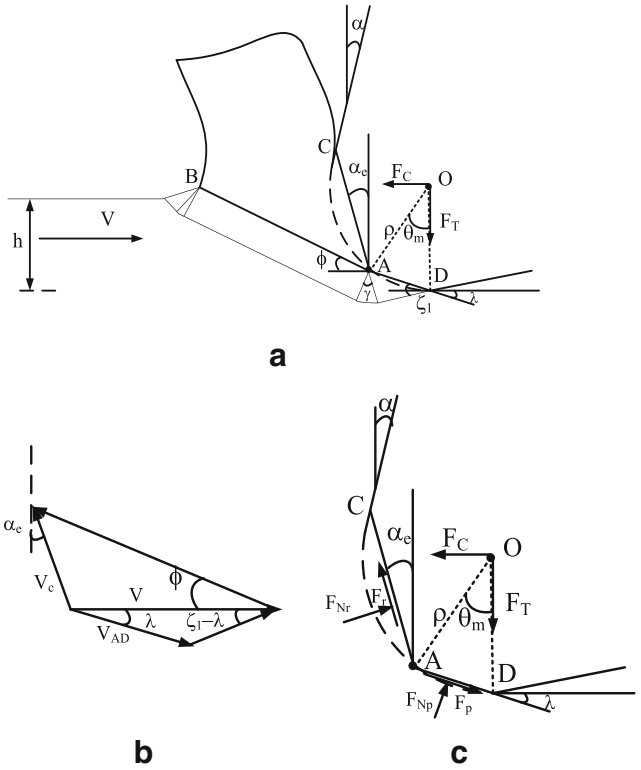

Fig. 3 **a** The slip-line field around the cutting tool edge [20]. **b** The hodograph of the slip-line field. **c** The normal and tangential forces acting on the cutting tool

2 Analytical micro-cutting model

In the process of the metal micro-cutting, the work-piece material experiences severe plastic deformation, and the ductile fracture occurs concurrently at the chip root, as shown in Fig. 1.

Figure 1 a shows that severe plastic deformation occurs before and after the grain is cut off. Also, it can be seen that the chip root contour is basically the same as the tool edge, which implies that built-up edge is not obvious in front of the cutting tool edge. In Fig. 1b, the phenomenon of material tearing can be observed. This work focuses on the case that no stable built-up edge generates or the size of it can be negligible, therefore, the micro-cutting process can be modeled as Fig. 2, incorporating the effects of both the radius of tool edge and the material separation.

In Fig. 2, A is the point on the edge radius at which the material separates. During the cutting process, the material above the point A forms the chip; whereas, that below is plowed under the edge to form the machined surface. New surfaces will be created due to the separation of the material. Therefore, the total work provided by the horizontal cutting force F_C is consumed by the following: (1) the plastic deformation of the work-piece material; (2) the friction between the work-piece and the tool surface; and (3) creation of the new surfaces [27].

In Fig. 2, ϕ denotes the shear angle, and the angle θ_m corresponds to the location of the point where the material separation occurs and ρ is the edge radius of the cutting tool. h is the uncut chip thickness which is the vertical distance between the bottom of cutting tool and the free surface of the work-piece, α is the rake angel, α_e is the effective rake angle which will be defined later. The vertical distance between point A on the edge radius and the bottom of the cutting tool can be expressed as:

$$h_{\min} = \rho(1-\cos\theta_m) \tag{1}$$

It is defined as minimum chip thickness in some literatures [30–34]. Therefore, the minimum chip thickness can be analyzed through determination of θ_m.

The slip-line field and its hodograph are shown in Fig. 3a and b, respectively, which are widely used in the analyses of cutting process [21]. Figure 3c shows the forces acting on the cutting tool with simplifying the curvilinear cutting edges as line segments.

Based on the slip-line field model, the cutting power related to the shearing, friction, and fracture can be derived as follows:

$$F_C V = \frac{\tau_y t V a \cos\alpha_e}{\sin\phi\cos(\phi+\alpha_e)} + \frac{F_r V \sin\phi}{\cos(\phi+\alpha_e)} + \frac{F_p V \sin(\zeta_1-\lambda)}{\sin(\zeta_1)} + RaV \tag{2}$$

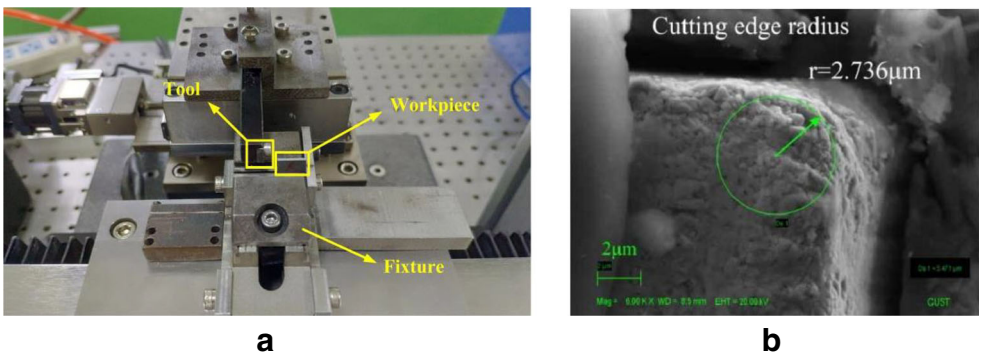

Fig. 4 **a** The set-up for orthogonal cutting. **b** SEM picture of the tool

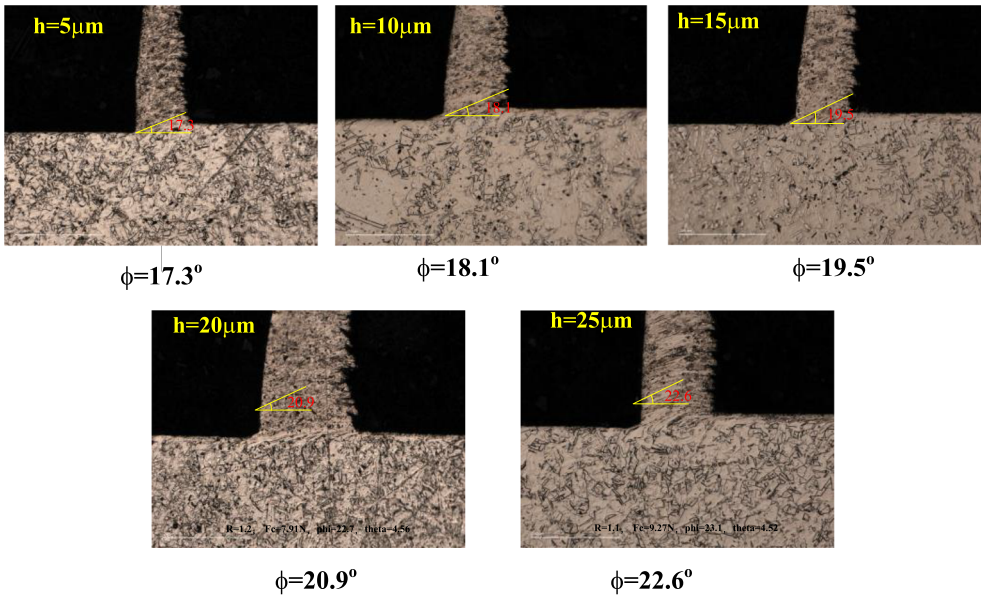

Fig. 5 SEM images of chip root and measurements of shear angles

In the equation, the first term on the right-hand side is the plastic work, the second and third term are the work related to the friction, and the last one is the work required to generate the new surfaces [27]. V is the cutting speed, t is the depth of cut, τ_y is the shear yield strength, a is the width of cut, R represents the fracture toughness of the work-piece material and α_e is the effective rake angle calculated as [11]:

$$\alpha_e = \begin{cases} \alpha \dfrac{h + \rho(\alpha_1 \cos\alpha - \sin\alpha - 1)}{h + \rho(\alpha_2 \cos\alpha - \sin\alpha - 1)} & h \geq \rho(1 + \sin\alpha) \\ \dfrac{1}{2}(\theta_t + \theta_c - \pi) & h < \rho(1 + \sin\alpha) \end{cases} \quad (3)$$

where

$$\alpha_1 = \frac{\alpha}{2} - \frac{\pi^2}{8\alpha} - \frac{\theta_c^2}{2\alpha} + \frac{\pi\theta_c}{2\alpha} \quad (4)$$

$$\alpha_2 = \alpha + \frac{\pi}{2} - \theta_c$$

$$\theta_t = \cos^{-1}\left(1 - \frac{h}{\rho}\right)$$

$$\theta_c = \cos^{-1}\left(1 - \frac{h_m}{\rho}\right) \quad (5)$$

Horizontal cutting force and surface tangential forces have the following relationship:

$$F_C = F_r \frac{\cos(\beta_r + \alpha_e)}{\sin\beta_r} + F_p \frac{\sin(\lambda + \beta_p)}{\sin\beta_p} \quad (6)$$

In Eq. (6), β_r and β_p are the friction angles at tool–chip and tool–work interfaces, respectively. ζ_1 is the slip-line angle related to the friction factor (m) at the tool–work-piece interface (AD) and can be determined according to slip-line field theory as

$$\zeta_1 = 0.5\cos^{-1}(m) \quad (7)$$

In slip-line filed theory the frictional stress is assumed constant and proportional to the material shear flow stress k:

$$\tau = m \cdot k \quad (8)$$

k is related to the uniaxial yield stress Y through the von Mises yield criterion

$$k = \frac{Y}{\sqrt{3}} \quad (9)$$

F_r is the friction force between the tool rake face and the work-piece. The friction angle β_p is determined as

Table 1 Measured values of shear angle and cutting force

Uncut chip thickness h (μm)	5	10	15	20	25
Shear angle (deg)	17.3	18.1	19.5	20.9	22.6
Cutting force Fc (N)	3.52	4.76	6.45	7.84	9.13

Table 2 Cutting conditions (m = 0.85 [29])

Rake angle (deg)	Width of cut (mm)	Edge radius (μm)	Friction angle (deg)	Shear yield stress (MPa)
0	1	2.7	40	70 [35]

$$\beta_{\mathrm{p}} = \tan^{-1}\left(\frac{\cos(2\zeta_1)}{1+\pi/2-2\xi+2\zeta_1-2\lambda+\sin(2\zeta_1)}\right)$$
$$\xi = \sin^{-1}\left(\frac{\sin(\lambda)}{\sqrt{2}\sin(\zeta_1)}\right) \quad (10)$$

The plowing force is:

$$F_p = m\tau_y l_{AD} a \quad (11)$$

Substituting Eqs. (6) and (11) into Eq. (2), one can obtain:

$$\frac{F_C}{\mathrm{a}} = \frac{\tau_y t\cos\alpha_e}{Q\sin\varphi\cos(\varphi+\alpha_e)} + \frac{m\tau_y l_{AD}}{Q} \times\left[\frac{\sin(\varsigma_1-\lambda)}{\sin(\varsigma_1)} - \frac{\sin(\lambda+\beta_p)\sin\beta_r\sin\varphi}{\sin\beta_p\cos(\beta_r+\alpha_e)\cos(\varphi+\alpha_e)}\right] + \frac{R}{Q} \quad (12)$$

where

$$\lambda = \theta_m/2 \ , \quad l_{AD} = 2\rho\sin\frac{\theta_m}{2} \ , \quad t = h-h_{\min} \quad (13)$$

$$Q = 1-\frac{\sin\beta_r\sin\phi}{\cos(\beta_r+\alpha_e)\cos(\phi+\alpha_e)} \quad (14)$$

According to the minimum energy principle, ϕ and θ_m should be such that the total power is the smallest, i.e., the first-order derivative of the total power with respect to ϕ or θ_m is zero ($\partial F_C/\partial\varphi = 0$, $\partial F_C/\partial\theta_m = 0$). Hence, two nonlinear equations can be obtained. By solving these two equations the effects of the cutting and material parameters to ϕ and θ_m can be analyzed.

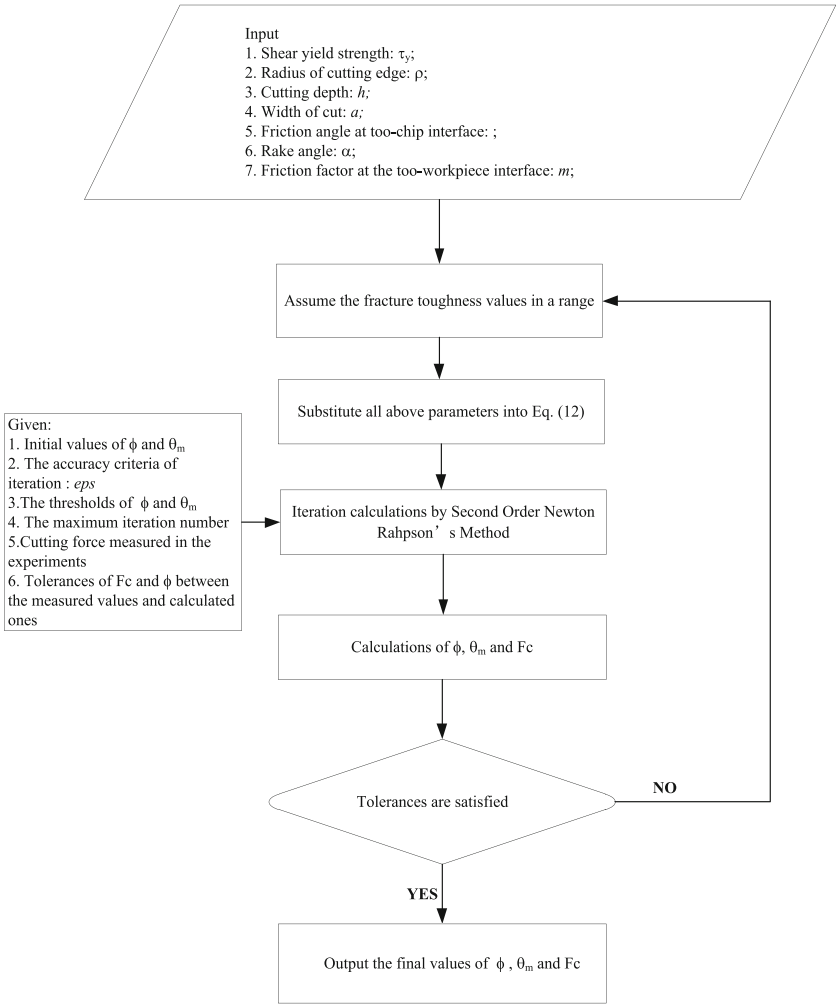

Fig. 6 Flowchart of the calculating procedure

3 Experimental validation and discussion

Experiments were carried out with oxygen-free copper (OFC) using uncoated tungsten carbide (WC) micro-cutting tool on the self-developed set-up for orthogonal cutting, as shown in Fig. 4a, and the cutting forces were measured with a table dynamometer (Kisler9256C).

The edge radius of the tool was observed to be approximately 2.7 μm, shown as Fig. 4b. The rake angle of the cutting tool is 0° and the clearance angle is 7°. Quick-stopping was performed to freeze the chip, and the shear angles were measured through the SEM images of the chip root using the microscope with super depth of field, shown in Fig. 5.

Table 1 shows the variations of the shear angle and the cutting force with the uncut chip thickness *h*.

The MATLAB program was developed to conduct the numerical computations based on the second-order Newton-Raphson method. In the analyses, the cutting parameters employed to solve ϕ and the θ_m are given, shown in Table 2. The specific calculating procedure is depicted in the flowchart demonstrated in Fig. 6 and the numerical results are shown in Fig. 7.

From Fig. 7a, it can be seen that the calculated cutting forces based on the proposed model are almost the same as the experimental results. Figure 7b illustrates the variation of shear angle versus the uncut chip thickness, and it demonstrates that there is only a little difference between the experimental measurements and the calculated results. Angle θ_m decreases with the uncut chip thickness increasing shown as Fig. 7c. However, the minimum chip thickness increases as shown in Fig. 7d. Figure 7e indicates that the fracture toughness varies within 1.1 to 1.4 kJ/m^2 corresponding to the variation of the uncut chip thickness within 5 to 25 μm. The fracture toughness value is also relatively low since oxygen-free copper is a soft material. The plowing forces were computed through Eq. (11); the results are shown in Fig. 7f, which

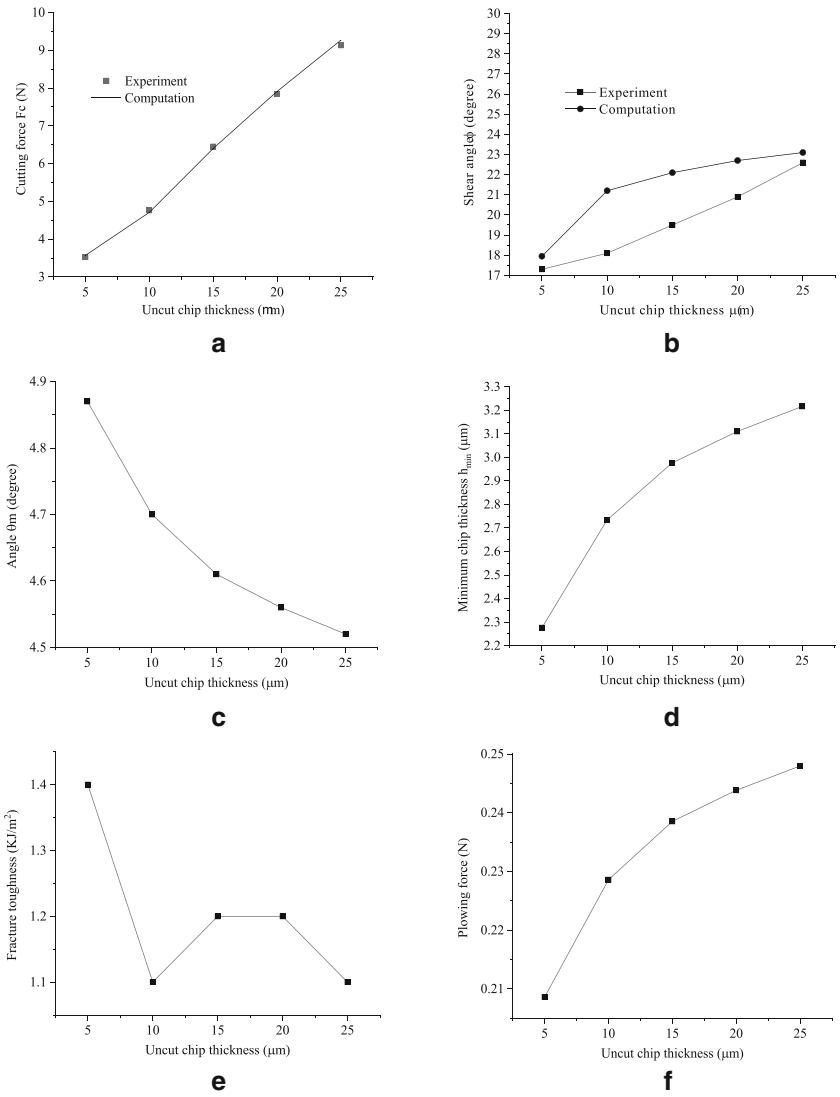

Fig. 7 **a** The comparison of cutting force (F_c) between calculating results and experimental measurements. **b** The computational and experimental results of the shear angle (Φ). **c** The variation of angle θm with uncut chip thickness. **d** The variation of minimum chip thickness (hmin) with uncut chip thickness. **e** The variation of fracture toughness with uncut chip thickness. **f** The variation of plowing force with uncut chip thickness

Table 3 Cutting conditions [29, 36] (m = 0.85)

Uncut chip thickness (mm)	Rake angle (deg)	Width of cut (mm)	Edge radius (μm)	Friction angle (deg)	Shear yield stress (MPa)
0.016	10	0.3	10	50	522
0.006	10	0.3	10	54.8	510

indicates that the plowing force increases with the uncut chip thickness.

Karpat [29] investigated the effect of edge radius on material separation for two cutting conditions using the experimental data given by Woon et al. [36], considering a stagnant metal zone in front of the cutting edge. The research work is of great significance to analyzing the process of micro-cutting with stable built-up edge (BUE). Nevertheless, under certain cutting conditions BUE can be avoided. In our series experiments obvious stable BUE were not observed. In order to compare our model with that proposed by Karpat [27], the calculations of shear angle and fracture toughness were performed using the same cutting parameters as listed in Table 3, and the calculating results are provided in Table 4.

In Table 4, the data of the shear angle and the fracture toughness in parentheses were the results in [29]. The shear angles obtained by our model are very close to those of Karpat's. However, the fracture toughness in our calculation is greater. It should be noticed that in Karpat's model the rake angle near the cutting tool tip is positive due to the BUE, but in our model it is always negative (see Fig. 3a), which leads to higher fracture toughness. This is also the major difference between the two models.

The effects of fracture toughness, shear yield strength, and friction angle to shear angle, material separation position, and cutting force in the micro-cutting process are investigated numerically as follows.

In the analyses, the uncut chip thickness is taken as 0.016 mm. The cutting force, shear angle, and the angle related to material separation point were calculated with the changes of fracture toughness, shear yield strength and friction angle, respectively. The results are drawn in Fig. 8.

Figure 8a, c, and e indicate that the cutting forces increase with all the three parameters. From Fig. 8b, it can be seen that with the increase of the fracture toughness, the shear angle ϕ decreases and the angle θ_m related to the material separation point increases, which imply that the chip formation becomes more difficult. When changing the shear yield stress from 500 MPa to 600 MPa with other parameters fixed, the shear angle ϕ increases and the angle θ_m decreases slightly (see Fig. 8d). The variation of θ_m is within 23.31°~23.13°, while ϕ varies from 22.67° to 23.58°.

In Fig. 8f, it can be seen that the friction angle influences the micro-cutting process greatly. The cutting force has a nonlinear relationship with the friction angle. Meanwhile, the changes of ϕ and θ_m are much larger than those in the cases of varying the fracture toughness and the shear yield stress. In practical cutting process cutting, fluid is often used to reduce the friction to lower the cutting force.

4 Conclusions

In this work, a micro-cutting model is developed based on the slip-line field theory considering the effects of cutting tool edge radius and material separation due to ductile fracture. The model proposed in this study focuses on the micro-cutting process with no stable built-up edge. This is its major difference from the model developed by Karpat [29], which deals with the micro-cutting process considering BUE in front of the cutting tool edge.

Based on the experimental data, the validation of the model was examined. The numerical results of the cutting forces and the shear angles agree with the experimental measurements very well, which indicates the model developed in this work is reasonable. Additionally, the minimum chip thickness can be determined using the model. The numerical investigations show that as the uncut chip thickness increases the shear angle increases, while the angle corresponding to the material separation point decreases. The minimum chip thickness increases slightly with the increases of uncut chip thickness. The plowing increases with uncut chip thickness.

Table 4 Calculating results

Uncut chip thickness (mm)	Shear angle ϕ (deg)	Mat. separation angle θ_m (deg)	Cutting force (N)	Fracture toughness (kJ/m^2)
0.016	22.99 (23.49)	23.15	16.39	17 (12)
0.006	17.99 (18.9)	13.73	8.85	13 (6.5)

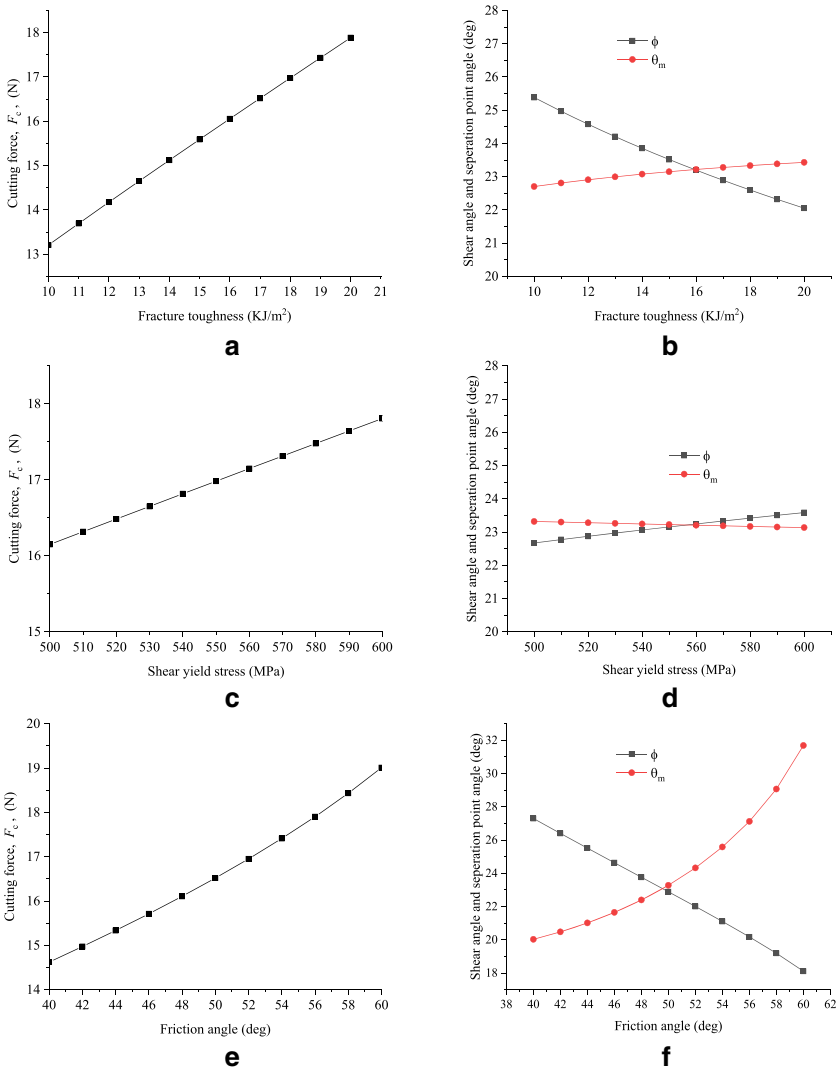

Fig. 8 **a** The effect of the fracture toughness to the cutting force (F_c). **b** The effect of the fracture toughness to the shear angle (Φ) and angle θ_m. **c** The relationship between the shear yield stress to the cutting force (F_c). **d** The influence of the shear yield stress to the shear angle (Φ) and angle θ_m. **e** The variation of the cutting force (F_c) with the friction angle. **f** The effect of the friction angle to the hear angle (Φ) and angle θ_m

Employing this model, the numerical investigations of the effects, the fracture toughness, the shear yield stress, and the friction to the micro-cutting process were performed. The results may be very helpful in selecting machining conditions and designing micro-cutting tools.

Authors' contributions Yiquan Li and Huadong Yu constructed the theoretical model. Jinkai Xu and Xiaozhou Li designed the experiment set-up. Measurements were performed by Zhanjiang Yu, Yiquan Li, and Jinkai Xu. Zhanjiang Yu developed the MATLAB program. The numerical analyses were performed by Zhanjiang Yu and Yiquan Li. Huadong Yu and Yiquan Li analyzed the data and contributed to writing the manuscript. Huadong Yu supervised the project and the collaboration.

Funding This work was supported by the National Key Research and Development Plan Project (No. 2018YFB1107403), the "111" Project of China (No. D17017), Jilin Province Scientific and Technological Development Program (No. 20190101005JH, No. 20180201057GX, No. 20190302076GX), and the Changchun Equipment and Technical Research Institute (WDZC2019JJ016).

Data availability The data that support the findings of this study are available from the corresponding authors upon reasonable request.

Compliance with ethical standards

Ethical approval Not applicable.

Consent to participate Not applicable.

Consent to publish Not applicable.

Competing interests The authors declare that they have no known competing financial interests.

References

1. Koç M, Özel T (eds) (2011) Micro-manufacturing: design and manufacturing of micro-products. John Wiley & Sons, Inc., Hoboken

2. Chae J, Park SS, Freiheit T (2006) Investigation of micro-cutting operations. Int J Mach Tools Manuf 46(3-4):313–332
3. Boswell B, Islam MN, Davies IJ (2018) A review of micro-mechanical cutting. Int J Adv Manuf Technol 94:789–806
4. Kim JD, Kim DS (1995) Theoretical analysis of micro-cutting characteristics in ultra-precision machining. J Mater Process Technol 49(3-4):387–398
5. Liu K, Melkote SN (2007) Finite element analysis of the influence of tool edge radius on size effect in orthogonal micro-cutting process. Int J Mech Sci 49(5):650–660
6. Lai X, Li H, Li C, Lin Z, Ni J (2008) Modelling and analysis of micro scale milling considering size effect, micro cutter edge radius and minimum chip thickness. Int J Mach Tools Manuf 48(1):1–14
7. Subbiah S, Melkote SN (2008) Effect of finite edge radius on ductile fracture ahead of the cutting tool edge in micro-cutting of Al2024-T3. Mater Sci Eng A 474(1-2):283–300
8. Afazov SM, Ratchev SM, Segal J (2010) Modelling and simulation of micro-milling cutting forces. J Mater Process Technol 210(15): 2154–2162
9. Vipindas K, Anand KN, Mathew J (2018) Effect of cutting edge radius on micro end milling: force analysis, surface roughness, and chip formation. Int J Adv Manuf Technol 97(1-4):711–722
10. Wu X, Li L, He N, Hao X, Yao C, Zhong L (2016) Investigation on the ploughing force in micro cutting considering the cutting edge radius. Int J Adv Manuf Technol 86(9-12):2441–2447
11. Jun MB, Goo C, Malekian M, Park S (2012) A new mechanistic approach for micro end milling force modeling. J Manuf Sci Eng 134(1):011006-1-9
12. An Q, Dang J, Liu G, Dong D, Ming W, Chen M (2019) A new method for deburring of servo valve core edge based on ultraprecision cutting with the designed monocrystalline diamond tool. Sci China Technol Sci 62(10):1805–1815
13. Schulze V, Autenrieth H, Deuchert M, Weule H (2010) Investigation of surface near residual stress states after micro-cutting by finite element simulation. CIRP Ann 59(1):117–120
14. Yang K, Liang YC, Zheng KN, Bai QS, Chen WQ (2011) Tool edge radius effect on cutting temperature in micro-end-milling process. Int J Adv Manuf Technol 52(9-12):905–912
15. Jin X, Altintas Y (2012) Prediction of micro-milling forces with finite element method. J Mater Process Technol 212(3):542–552
16. Thepsonthi T, Özel T (2015) 3-D finite element process simulation of micro-end milling Ti-6Al-4V titanium alloy: experimental validations on chip flow and tool wear. J Mater Process Technol 221: 128–145
17. Wu J, Liu Z (2010) Modeling of flow stress in orthogonal micro-cutting process based on strain gradient plasticity theory. Int J Adv Manuf Technol 46(1-4):143–149
18. Emamian A (2018) The effect of tool edge radius on cutting conditions based on updated Lagrangian formulation in finite element method (Doctoral dissertation).
19. Shi Z, Li Y, Liu Z, Qiao Y (2018) Determination of minimum uncut chip thickness during micro-end milling Inconel 718 with acoustic emission signals and FEM simulation. Int J Adv Manuf Technol 98(1-4):37–45
20. Annoni M, Biella G, Rebaioli L, Semeraro Q (2013) Microcutting force prediction by means of a slip-line field force model. Procedia CIRP 8:558–563
21. Waldorf DJ, DeVor RE, Kapoor SG (1998) A slip-line field for ploughing during orthogonal cutting. J Manuf Sci Eng 120(4): 693–699
22. Jin X, Altintas Y (2011) Slip-line field model of micro-cutting process with round tool edge effect. J Mater Process Technol 211(3):339–355
23. Fang N (2003) Slip-line modeling of machining with a rounded-edge tool—part I: new model and theory. J Mech Phys Solids 51(4): 715–742
24. Fang N (2003) Slip-line modeling of machining with a rounded-edge tool—part II: analysis of the size effect and the shear strain-rate. J Mech Phys Solids 51(4):743–762
25. Shaw MC, Cookson JO (2005) Metal cutting principles, vol 2. Oxford university press, New York
26. Heald PT, Spink GM, Worthington PJ (1972) Post yield fracture mechanics. Mater Sci Eng 10:129–138
27. Atkins AG (2003) Modelling metal cutting using modern ductile fracture mechanics: quantitative explanations for some longstanding problems. Int J Mech Sci 45(2):373–396
28. Merchant ME (1945) Mechanics of the metal cutting process. I. Orthogonal cutting and a type 2 chip. J Appl Phys 16(5):267–275
29. Karpat Y (2009) Investigation of the effect of cutting tool edge radius on material separation due to ductile fracture in machining. Int J Mech Sci 51(7):541–546
30. Subbiah S (2006) Some investigations of scaling effects in micro-cutting (Doctoral dissertation, Georgia Institute of Technology).
31. Basuray PK, Misra BK, Lal GK (1977) Transition from ploughing to cutting during machining with blunt tools. Wear 43(3):341–349
32. Son SM, Lim HS, Ahn JH (2005) Effects of the friction coefficient on the minimum cutting thickness in micro cutting. Int J Mach Tools Manuf 45(4-5):529–535
33. Malekian M, Mostofa MG, Park SS, Jun MBG (2012) Modeling of minimum uncut chip thickness in micro machining of aluminum. J Mater Process Technol 212(3):553–559
34. Yuan ZJ, Zhou M, Dong S (1996) Effect of diamond tool sharpness on minimum cutting thickness and cutting surface integrity in ultraprecision machining. J Mater Process Technol 62(4):327–330
35. Olsson M, Bushlya V, Zhou J, Ståhl J (2016) Effect of feed on subsurface deformation and yield strength of oxygen-free pitch copper in machining. Procedia CIRP 45:103–106
36. Woon KS, Rahman M, Neo KS, Liu K (2008) The effect of tool edge radius on the contact phenomenon of tool-based micromachining. Int J Mach Tools Manuf 48(12-13):1395–1407